

Rapid Communication

Molecular electron paramagnetic resonance imaging of melanin in melanomas: a proof-of-concept

Emilia Vanea,^{1†} Nicolas Charlier,^{1†} Julie DeWever,² Mustapha Dingizli,¹ Olivier Feron,² Jean-François Baurain³ and Bernard Gallez^{1*}

¹Biomedical Magnetic Resonance Unit, Université Catholique de Louvain, UCL, Brussels, Belgium

²Pharmacotherapy Unit, Université Catholique de Louvain, UCL, Brussels, Belgium

³Medical Oncology Unit, Université Catholique de Louvain, UCL, Brussels, Belgium

Received 21 September 2007; Revised 29 November 2007; Accepted 29 November 2007

ABSTRACT: The incidence of malignant melanoma is increasing at an alarming rate. As the clinical outcome of the disease strongly depends on the localization of the lesion, early detection at the initial stages of development is critical. Here, we suggest spatial characterization of melanoma based on the presence of endogenous stable free radicals in melanin pigments. Taking into account the abundance of these naturally occurring free radicals in proliferating melanocytes and their localization pattern, we hypothesized that electron paramagnetic resonance (EPR) imaging could be a unique tool for mapping melanomas with high sensitivity and high resolution. The potential of EPR to image melanoma samples was demonstrated *in vitro* in animal and human samples. Using EPR systems operating at low frequency, we were also able to record *in vivo* EPR spectra and images from the melanin present in a subcutaneous melanoma implanted in a mouse. In addition to the proof-of-concept and the achievement of providing the first non-invasive image of an endogenous radical, this technology may represent a key advance in improving the diagnosis of suspected melanoma lesions. Copyright © 2008 John Wiley & Sons, Ltd.

KEYWORDS: electron paramagnetic resonance (EPR); EPR imaging; *in vivo* EPR; melanoma

INTRODUCTION

The incidence of malignant melanoma is increasing at an alarming rate. The National Cancer Institute expects 60 000 new cases of melanoma in the United States in 2007; among these cases, about 8100 deaths will occur. The clinical outcome of the disease depends on the localization of the lesion, as the estimated 5-year survival rate is about 100% for superficial melanoma diagnosed early, but less than 10% for melanoma that has disseminated to major organs (lungs, brain). Early

detection at the initial stages of development is, therefore, critical for favorable outcomes. New imaging modalities potentially offer the ability to characterize melanomas non-invasively. Unfortunately, optical techniques are limited by depth penetration into the skin, whereas other imaging methods (computed tomography, MRI) are limited by their weak contrast and specificity to detect such lesions.

In the skin, melanin is produced by melanocytes spread throughout the lower part of the epidermis or that have grown in clusters (naevi). Melanoma occurs when melanocytes become malignant. When it is suspected that a primary lesion may be a melanoma, biopsy is performed for staging and management. Essential prognostic factors include the Breslow index (lesion thickness) and Clark's level (invasion depth). When downward growth has occurred, the disease often metastasizes to other parts of the body.

Here, we suggest spatial characterization of melanoma based on the presence of endogenous stable free radicals in melanin pigments. Melanins are polymeric pigments that contain a mixture of eumelanin and pheomelanin. In melanoma, eumelanin is the major component of the pigment mixture (1). The melanin pigments can be detected by electron paramagnetic resonance (EPR) spectroscopy

*Correspondence to: B. Gallez, CMFA/REMA, Université Catholique de Louvain, Avenue Mounier 73.40, B-1200 Brussels, Belgium.

E-mail: bernard.gallez@uclouvain.be

[†]These authors contributed equally to this work.

Contract/grant sponsor: Belgian National Fund for Scientific Research (FNRS).

Contract/grant sponsor: Televie.

Contract/grant sponsor: Fonds Joseph Maisin.

Contract/grant sponsor: Saint-Luc Foundation.

Contract/grant sponsor: Actions de Recherches Concertées-Communauté Française de Belgique; contract/grant number: ARC 04/09-317.

Contract/grant sponsor: Pôle d'attraction Interuniversitaire; contract/grant number: PAI VI (P6/38).

Abbreviations used: 2D, two-dimensional; 3D, three-dimensional; EPR, electron paramagnetic resonance; EPRI, electron paramagnetic resonance imaging.

(2,3), a magnetic-resonance-based technique that detects species with unpaired electrons. With the use of appropriate field gradients, EPR imaging (EPRI) can map the distribution of free radicals inside tissues (4). At room or body temperature, the EPR signal from melanin complexes present in melanomas is characterized by a single narrow line, with a g value of 2.005 (constant characteristic of the chemical species, analogous to the NMR chemical shift) (Fig. 1a). It has been demonstrated that the EPR signal intensity correlates with the number of melanin granules in melanomas (5). Taking into account the abundance of these naturally occurring free radicals in proliferating melanocytes and their localization pattern, we hypothesized that EPRI could be a unique tool for mapping melanomas with high sensitivity and high resolution.

MATERIALS AND METHODS

Mice and tumor models

All experiments were conducted according to national animal care regulations. C57BL/6 mice were purchased from The Jackson Laboratory (Bar Harbor, ME, USA) at 6–8 weeks of age. Mice anesthetized with isoflurane (2% for induction, 0.8% for maintenance) were subcutaneously or intravenously (for pulmonary metastasis) injected with 10^6 syngenic B16 melanoma cells (ATCC, Menassas, VA, USA) 12 and 17 days, respectively, before the experiments. For *in vitro* studies, mice were killed by cervical dislocation, and the tumor core (500 μm thick) or the lungs were excised and freeze-dried or directly examined. For imaging, samples were placed in a quartz tube (internal diameter 9 mm) in the resonator cavity. For *in vivo* studies, the subcutaneous injection of B16 melanoma was performed on the top of the mouse's head to minimize motion artifacts.

Human melanomas

Slices ($\sim 500 \mu\text{m}$ thick) from paraffin-embedded blocks were collected and put in a flat quartz tissue-cell before being put in the resonator cavity. A contiguous slide (5 μm thick) was processed for histology (hematoxylin & eosin staining).

EPR spectroscopy and imaging

In vitro spectra and images were recorded using a commercial Elexsys imaging system from Bruker (Rheinstetten, Germany) with an X-band microwave bridge working at ~ 9.7 GHz and equipped with an Elexsys Super High Sensitivity Probehead. The typical acquisition parameters for the *in vitro* studies were: center field, 343 mT; modulation amplitude, 0.8 mT; modulation

frequency, 100 kHz; power, 10 mW. When used, the gradient was 4.9 mT/cm.

In vivo spectra were recorded using a commercial EPR spectrometer (Magnetech, Berlin, Germany) with a low-frequency microwave bridge operating at 1.2 GHz and an extended loop resonator. Acquisition parameters were: center field, 53 mT; sweep width, 10 mT; modulation amplitude, 0.42 mT; modulation frequency, 100 kHz; power, 95 mW. *In vivo* images were recorded using an Elexsys imaging system from Bruker with an L-band microwave bridge working at 1.1 GHz, and equipped with an E540R23 L-Band EPR head-coil resonator (internal diameter 2.3 cm). Acquisition parameters for two-dimensional (2D) imaging in the zx plane were: center field, 39.50 mT; sweep width, 13.50 mT; modulation amplitude, 0.335 mT; modulation frequency, 100 kHz; power, 45 mW; gradient, 1 mT/cm.

RESULTS AND DISCUSSION

The potential of EPR to image melanoma samples was first assessed *in vitro* using standard EPR systems operating at 9 GHz. At this frequency, non-resonant absorption by water could prevent measurement. To avoid this problem, melanoma B16 samples, which were grown subcutaneously in C57BL/6 mice, were surgically removed and freeze-dried before the EPR measurement. Using appropriate field gradients, it was possible to obtain 2D images of the melanomas with high resolution (250 μm /pixel) (Fig. 1b). The application of gradients in three directions provided the volume of the tumor in three dimensions (Fig. 1c). To exclude a possible contribution of radicals generated during the freeze-drying process, EPRI was applied on fresh melanoma tissue slices ($\sim 500 \mu\text{m}$ thick) after insertion of the sample inside a quartz tissue-cell. In Fig. 1d,e, it can be seen that the EPR image can clearly delineate the surface of the melanoma slice under investigation. As a model of melanoma metastases, we used lungs from mice previously injected with B16 melanoma cells. Macroscopically, areas of the lungs colonized by the melanoma cells are visible as brown spots due to the presence of melanin pigments (Fig. 1f). These lung metastases were clearly localized using 2D and three-dimensional (3D) EPRI (Fig. 1g and Fig. 1h, respectively).

To assess the relevance of our technique in delineating human melanomas, we applied the method to five paraffin-embedded melanomas excised from patients. EPRI was able to delineate the areas with proliferation of melanocytic cells. As an illustrative example, we present in Fig. 2 a melanoma metastasis with irregular clusters of melanocytes present in the derma of a patient. It can be observed that the EPR image obtained is comparable to the histological section. Note that the slices investigated were contiguous, with different slice thicknesses (500 μm for the slice imaged by EPR, 5 μm for the histological

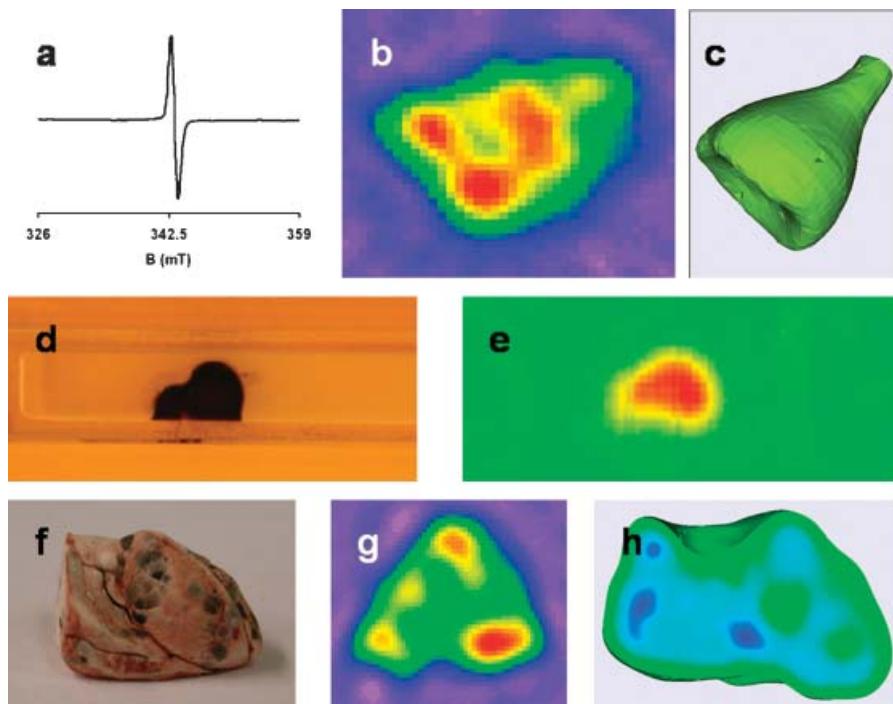


Figure 1. *In vitro* EPR spectra and images from melanoma B16. (a) Spectrum from a freeze-dried melanoma. (b,c) 2D image (b) and 3D image (c) from a freeze-dried melanoma. (d,e) Picture from a fresh melanoma slice (d) and the corresponding EPR image (e). (f–h) Melanoma B16 metastases in the lungs of mice: picture of freeze-dried lungs with metastases (f), 2D transversal EPR image (g), and longitudinal section through a 3D EPR image (h).

slice), explaining the slight differences between the EPRI projection of melanin content and the histological image.

A key issue in the future will be to transfer this technique to an *in vivo* clinical situation. Spectrometers operating at low frequency have been developed recently,

allowing higher penetration of the wave into the tissues (1 cm depth penetration at 1 GHz, several centimeters at 300 MHz). Using EPR systems operating at 1.1 GHz, we were able to record *in vivo* EPR spectra from the melanin present in a subcutaneous melanoma implanted in a

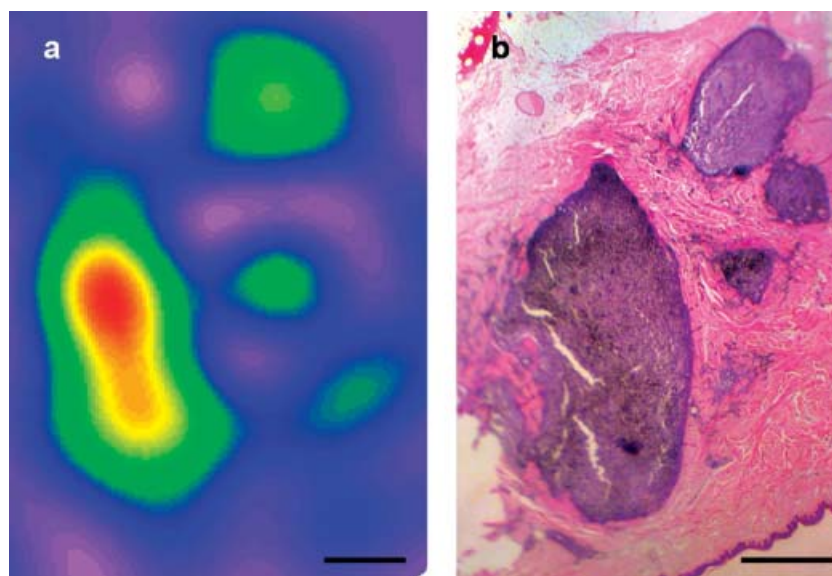


Figure 2. *In vitro* images of cross-sections through paraffin-embedded human metastases. (a) 2D EPR image through a section of thickness 500 μm . (b) Histological section (5 μm thick) from a contiguous slice. Scale bars: 1 mm.

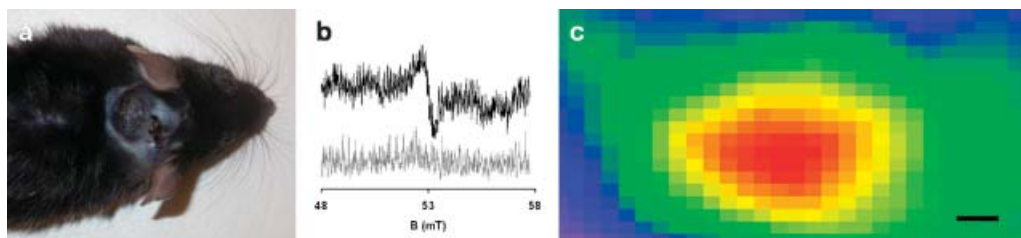


Figure 3. *In vivo* studies on B16 melanoma in mice. (a) Melanoma grown in subcutaneous tissue. (b) *In vivo* EPR spectra obtained with a low-frequency EPR spectrometer with a surface coil placed over the melanoma (top) or on the head of a mouse without melanoma (bottom). (c) *In vivo* EPR image obtained from the melanoma using a head-coil loop-gap resonator. Scale bar: 2 mm.

mouse (Fig. 3a). The EPR spectrum was unambiguously ascribed to melanin (Fig. 3b), as the signal was absent when EPR spectra were recorded from control mice without melanoma in the same experimental conditions (Fig. 3b). Finally, we recorded an *in vivo* EPR image from this melanoma (Fig. 3c). This result is the first direct, non-invasive *in vivo* image of a naturally occurring free radical. So far, *in vivo* EPR has been limited to the detection of administered stable free radicals used as indicators of the local environment [oxygen, pH, microviscosity, redox status (6–12)], or of stable radical spin adducts formed after reaction of reactive species with administered spin traps (13).

In addition to the proof-of-concept and the achievement of providing the first non-invasive image of an endogenous radical, the present technology could represent a key advance in improving the diagnosis of suspected melanoma lesions. During the last few years, unprecedented progress has been made in *in vivo* EPR technology and applications (14). The first clinical EPR spectrometer has been built recently and pioneer studies conducted in humans (15,16). These technological developments combined with our present findings may open the way for improved early diagnosis of melanomas using whole-body EPR magnets and surface coils placed over suspect lesions. Further work is needed to optimize EPRI systems for the detection of melanomas in humans, including the development of convenient gradient coils and resonators, and optimization of the signal-to-noise ratio by defining the optimal frequency for recording the EPR data. We anticipate that our concept could be applied as a non-invasive method to delineate the melanocyte proliferation area before biopsy (avoiding the need for a second intervention in the case of partial exeresis), and as a simple means of sorting suspect lesions based on lesion thickness and invasion depth. It is expected that moles could be easily differentiated from melanoma on the basis of downward growth (lesion thickness and invasion depth into the skin). It would also be interesting to investigate whether the method could also help in the differentiation between melanoma types. For example, amelanotic melanomas could be used as negative controls, because of the expected absence of signal from these melanoma types. With further improvements to resolve the problem

of depth penetration, a future application could be the non-invasive detection of lymph node invasion and distant metastases.

Acknowledgements

This work is supported by grants from the Belgian National Fund for Scientific Research (FNRS), the Télévie, the Fonds Joseph Maisin, the Saint-Luc Foundation, the ‘Actions de Recherches Concertées-Communauté Française de Belgique-ARC 04/09-317’, and the ‘Pôle d’attraction Interuniversitaire PAI VI (P6/38)’.

REFERENCES

- Ito S, Jimbow K. Quantitative analysis of eumelanin and pheomelanin in hair and melanomas. *J. Invest. Dermatol.* 1983; **80**: 268–272.
- Sealy RC, Hyde JS, Felix CC, Menon IA, Prota G. Eumelanins and pheomelanins: characterization by electron spin resonance spectroscopy. *Science* 1982; **217**: 545–547.
- Enochs MS, Nilges MJ, Swartz HM. A standardized test for the identification and characterization of melanins using electron paramagnetic resonance (EPR) spectroscopy. *Pigment Cell Res.* 1993; **6**: 91–99.
- Berliner LJ, Fujii H. Magnetic resonance imaging of biological specimens by electron paramagnetic resonance of nitroxide spin labels. *Science* 1985; **227**: 517–519.
- Elek G, Lapis K, Rockenbauer A. ESR investigation of paraffin-embedded ocular melanomas. *Br. J. Cancer* 1980; **41**: 199–203.
- Liu KJ, Gast P, Moussavi, Norby SW, Vahidi N, Walczak T, Wu M, Swartz HM. Lithium phthalocyanine: a probe for electron paramagnetic resonance oximetry in viable biological systems. *Proc. Natl. Acad. Sci. USA* 1993; **90**: 5438–5442.
- He G, Shankar RA, Chzhan M, Samouilov A, Kuppusamy P, Zweier JL. Noninvasive measurement of anatomic structure and intraluminal oxygenation in the gastrointestinal tract of living mice with spatial and spectral EPR imaging. *Proc. Natl. Acad. Sci. USA* 1999; **96**: 4586–4591.
- Gallez B, Baudelet C, Jordan BF. Assessment of tumor oxygenation by electron paramagnetic resonance: principles and applications. *NMR Biomed.* 2004; **17**: 240–262.
- Matsumoto K, Hyodo F, Matsumoto A, Koretsky AP, Sowers AL, Mitchell JB, Krishna MC. High-resolution mapping of tumor redox status by magnetic resonance imaging using nitroxides as redox-sensitive contrast agents. *Clin. Cancer Res.* 2006; **12**: 2455–2462.
- Hyodo F, Matsumoto K, Matsumoto A, Mitchell JB, Krishna MC. Probing the intracellular redox status of tumors with magnetic

- resonance imaging and redox-sensitive contrast agents. *Cancer Res.* 2006; **66**: 9921–9928.
11. Gallez B, Mäder K, Swartz HM. Noninvasive measurement of the pH inside the gut by using pH-sensitive nitroxides. *An in vivo EPR study. Magn. Reson. Med.* 1996; **36**: 694–697.
 12. Halpern HJ, Chandramouli GV, Barth ED, Yu C, Peric M, Grdina DJ, Teicher BA. Diminished aqueous microviscosity of tumors in murine models measured with *in vivo* radiofrequency electron paramagnetic resonance. *Cancer Res.* 1999; **59**: 5836–5841.
 13. Yoshimura T, Yokoyama H, Fujii S, Takayama F, Oikawa K, Kamada H. *In vivo* EPR detection and imaging of endogenous nitric oxide in lipopolysaccharide-treated mice. *Nat. Biotechnol.* 1996; **14**: 992–994.
 14. Gallez B, Swartz HM. *In vivo* EPR: when, how and why? *NMR Biomed.* 2004; **17**: 223–225.
 15. Swartz HM, Khan N, Buckley J, Comi R, Gould L, Grinberg O, Hartford A, Hopf H, Hou H, Hug E, Iwasaki A, Lesniewski P, Salikhov I, Walczak T. Clinical applications of EPR: overview and perspectives. *NMR Biomed.* 2004; **17**: 335–351.
 16. Salikhov I, Walczak T, Lesniewski P, Khan N, Iwasaki A, Comi R, Buckley J, Swartz HM. EPR spectrometer for clinical applications. *Magn. Reson. Med.* 2005; **54**: 1317–1320.